THE GEOLOGICAL SOCIETY OF AMERICA®

Emergence of wet conditions in the Mono Basin of the Western USA coincident with inception of the Last Glaciation

Guleed A.H. Ali[1,†], Ke Lin[1,2], Sidney R. Hemming[3,4], Stephen E. Cox[4], Philipp Ruprecht[5], Susan R.H. Zimmerman[6], Scott Stine[7], and Xianfeng Wang[1,2]

[1]*Earth Observatory of Singapore, Nanyang Technological University, 50 Nanyang Avenue, Block N2-01a-15, Singapore 639798*
[2]*Asian School of the Environment, Nanyang Technological University, 50 Nanyang Avenue, Block N2-01C-63, Singapore 639798*
[3]*Department of Earth and Environmental Sciences, Columbia University, 557 Schermerhorn Extension, 1200 Amsterdam Avenue, New York, New York 10027, USA*
[4]*Lamont-Doherty Earth Observatory, 61 Route 9W, Palisades, New York 10964, USA*
[5]*Department of Geological Sciences and Engineering, University of Nevada, Reno, 1664 North Virginia Street, Reno, Nevada 89557, USA*
[6]*Center for Accelerator Mass Spectrometry, Lawrence Livermore National Laboratory, 7000 East Avenue, Livermore, California 94550, USA*
[7]*Anthropology, Geography, and Environmental Studies, California State University, East Bay, 25800 Carlos Bee Boulevard, Robinson Hall (Room) 211, Hayward, California 94542, USA*

ABSTRACT

At present, the Basin and Range of the western USA is arid, but geologic studies show evidence of past wetness. The timing of these wetter conditions reveals a close association with glacial conditions. This association has led to the hypothesis of a causal link between glacial climate and regional wetness, but poor age control on the onset of regional wetness thwarts a test of this hypothesis. Here we determine the start of the most recent interval of persistent wetness in the Mono Basin, which is a hydrologically closed depression that sits at the west-central edge of the Basin and Range. The most recent emergence of persistent wetness in the Mono Basin is stratigraphically correlated with the depositional age of Ash 19—a rhyolitic ash bed that represents the oldest tephra of the Wilson Creek Formation and one of the earliest-known products of explosive volcanic activity from the Mono Craters. We constrain the depositional age of Ash 19 by using the U/Th disequilibrium dating method to date carbonates that are younger and older than Ash 19. Our U/Th dating results show that Ash 19 was deposited before the formation of a cross-cutting carbonate bed dated to 69.2 ± 0.3 ka but after an underlying carbonate tufa dated to 67.4 ± 3.5 ka, which suggests that the start of wetness in the Mono Basin was contemporary with the inception of the Last Glaciation—the beginning of Marine Isotope Stage 4—at ca. 70 ka. This finding corroborates the hypothesis of a link between glacial climate and regional wetness.

INTRODUCTION

The landscape of the western United States has been shaped by an interplay between tectonics and climate. Over the last 30 m.y., rifting has stretched the region between the Sierra Nevada and the Colorado Plateau, fracturing and extending a tableland into a series of valleys and mountain ranges known as the Basin and Range (Colgan and Henry, 2009; Dickinson, 2013; Long, 2019). Further shaping this tectonically stretched terrain is the arid to semi-arid hydroclimate of the present. This aridity, however, has not been persistent over geologic timescales. Geologic studies show that regional hydroclimate varied between dry and wet intervals. Researchers from the late nineteenth century first deduced these wet intervals from the stratigraphic and geomorphic fingerprints of vast lakes, which filled valleys that are desiccated today (Fig. 1; e.g., Russell, 1884, 1895; Gilbert, 1890). It was reasoned that the evidence of unusually wet conditions across the region required a reorganization of atmospheric circulation, and the timing of the reorganization was hypothesized to correlate with intervals of glaciation (Antevs, 1952). This hypothesis agrees with the results of radiometric dating studies, which show that the most recent interval of large lakes ended at about the time of the last glacial termination (e.g., Oviatt, 2015; Adams and Rhodes, 2019). However, a robust test of the hypothesized link between regional wetness and glacial climate remains hindered by uncertainty about when the most recent wet interval started (e.g., Oviatt and McCoy, 1992). Here, we present new data that robustly dates an exposed flooding surface of Mono Lake and suggest that the beginning of the most recent wet interval in the Mono Basin, California, USA, coincided with the last glacial inception.

The Start of the Most Recent Wet Interval in the Mono Basin, California

The Mono Basin is a tectonically active depression that is bounded on its west by the steep eastern escarpment of the Sierra Nevada, on its north by the Bodie Hills, on its east by the Anchorite Hills, on its southeast by Cowtrack Mountain, and on its south by the rim of the Long Valley Caldera (Gilbert et al., 1968; Bailey, 2004; Fig. 2). The basin is also hydrologically closed (Lajoie, 1968). This hydrologically closed arrangement permits the fluctuations of the basin's enclosed lake, Mono Lake, to be used as a proxy for hydroclimate (Benson and Paillet, 1989).

A past interval of greater wetness in the Mono Basin is inferred from its geomorphology and stratigraphy (Russell, 1889; Lajoie, 1968). The geomorphic evidence includes wave-cut terraces, deltas, and littoral embankments that are found up to 200 m above the 1945 m level of the present lake (Russell, 1889). Consistent with these geomorphic indicators of a larger Mono

†guleed.ahmed@ntu.edu.sg.

GSA Bulletin;
published online 2 February 2022

https://doi.org/10.1130/B36084.1; 13 figures; 1 table; 1 supplemental file.

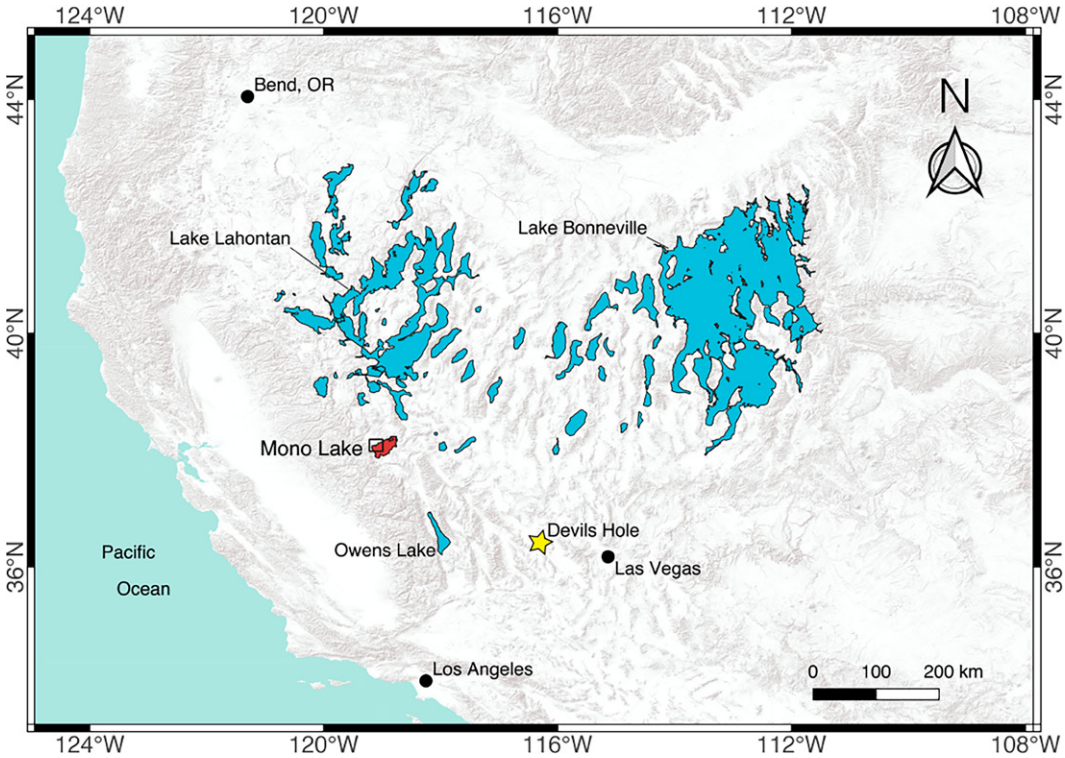

Figure 1. Digital elevation model map of the western United States shows high-stand surface areas of lakes that filled valleys of the Basin and Range during the Late Pleistocene (blue). The work of this study took place on the ancient Mono Lake (red color). Approximate area shown in Figure 2 is highlighted by the box outlined in black.

Lake are the sedimentary sequences exposed along the walls of stream-cut canyons, which are described and unified in the Ph.D. thesis of Lajoie (1968) as the Wilson Creek Formation. At its type locality along lower Wilson Creek canyon, which is ~30 m above the present lake, the Wilson Creek Formation stratotype comprises 10–14 m of lacustrine silts intercalated with 19 tephra layers whose volcanic sources include the intrabasin Mono Craters and Black Point in addition to the extrabasin Mammoth Mountain (Marcaida et al., 2014). These 19 tephra layers are numerically named by their reverse depositional order (Fig. 3). Ash 19 is the oldest, and Ash 1 is the youngest. This sequence of

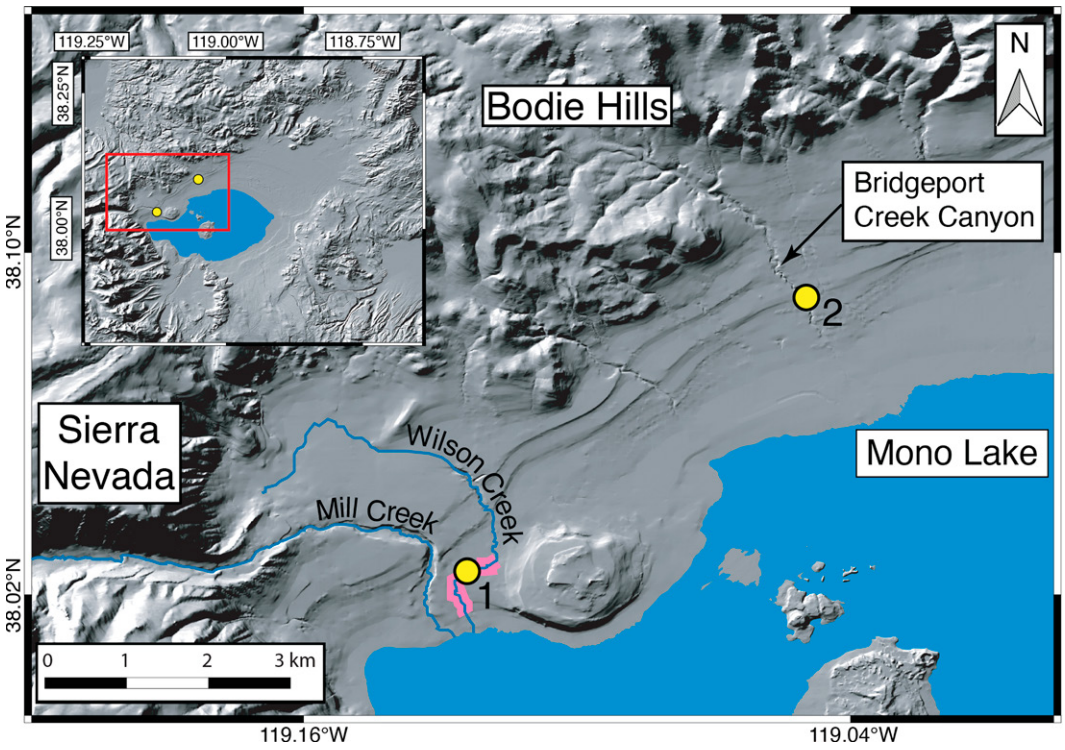

Figure 2. Digital elevation model map shows the northwest Mono Basin. Footprint of modern Mono Lake is shown in blue (lake surface elevation is ~1945 m). The northern edge of the Mono Basin is defined by the Bodie Hills. The Sierra Nevada marks the western limit of the basin. Sediments exposed along the lower stretch of Wilson Creek (highlighted in pink) constitute the type section of the Wilson Creek Formation. Locations marked by yellow circles and labeled with numbers 1 and 2 indicate sites where we measured sedimentary sections and sampled carbonates associated with Ash 19 of the Wilson Creek Formation. Site 1 is our "Tufa site" (~1987 m). Site 2 marks the location of our "Between site" (~2010 m) and the location of IV D (~2006 m) of Lajoie (1968). Inset map in the upper-left corner shows the entire Mono Basin. The red box in the inset map shows the limits of the main figure.

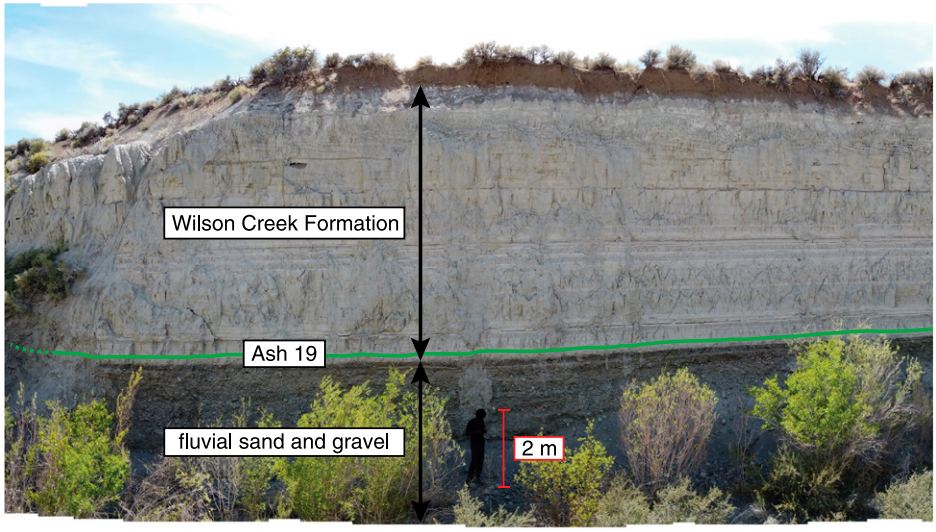

Figure 3. Photograph looks toward the western canyon wall of lower Wilson Creek. The sediments exposed along this canyon wall constitute a lake transgressive sequence. This sequence is represented by fluvial gravels that are overlain by lacustrine silts of the Wilson Creek Formation. The silts contain 19 tephra beds (note: the youngest two tephra beds are eroded from the site photographed here). The oldest tephra bed, Ash 19, which is highlighted by the blue-green line (dashed where covered), is deposited no more than a few centimeters above the contact between the lacustrine silts and fluvial gravel.

lacustrine silts and tephra is underlain by fluvial gravels and overlain by a veneer of aeolian and littoral sands, which suggests that the deposition of the Wilson Creek Formation coincided with a sustained interval of unusual wetness whose onset is marked by the contact between the fluvial gravels and lacustrine silts. This contact represents a wave-cut surface that was flooded by Mono Lake (Fig. 4). The age of this paleo-flooding surface is closely approximated by the oldest Wilson Creek Formation tephra, Ash 19, for it is contained in silts that lie no more than a few centimeters above the paleo-flooding surface. Hence, the depositional age of Ash 19 constrains the most recent emergence of sustained wetter conditions in the Mono Basin.

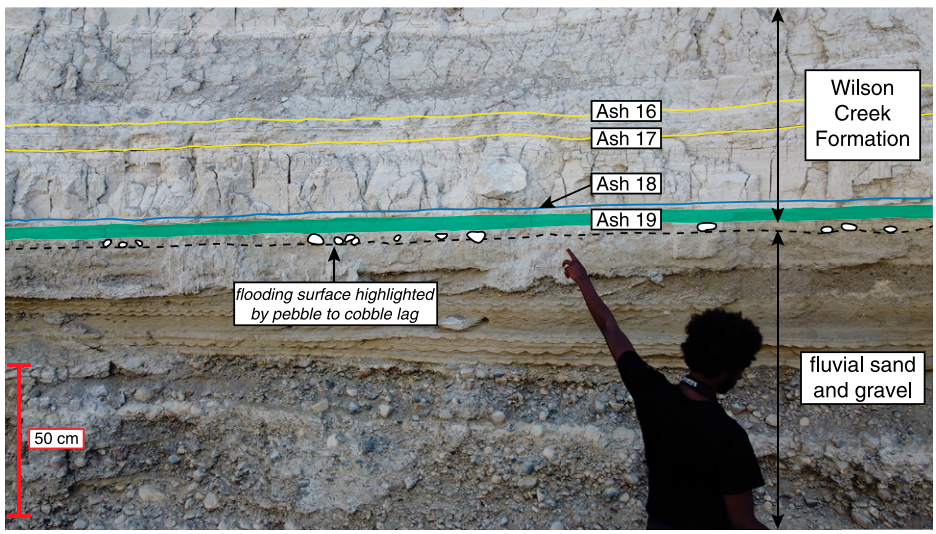

Figure 4. Photo of the western canyon wall of Wilson Creek shows the fluvial strata that underlie the lacustrine silts of the Wilson Creek Formation. The contact between the fluvial and lacustrine deposits represents a paleo-surface across which Mono Lake flooded (black dashed line). The flooding surface constrains the timing of a hydroclimatic change between conditions that sustained a lower lake before the Wilson Creek Formation to that which supported a higher lake for the duration of the Wilson Creek Formation (Lajoie, 1968). The age of this hydroclimatic change is most closely approximated by the depositional age of Ash 19 (blue-green).

Disagreement on the Depositional Age of Ash 19

Debate on the depositional age of Ash 19 prevents a determination of the beginning of the most recent wet interval in the Mono Basin. Age estimates from direct and indirect dating methods vary between 90 ka and 27 ka (Fig. 5). Indirect estimates are derived from Wilson Creek Formation age models and interpreted paleomagnetic correlations between the Wilson Creek Formation and marine sedimentary records. Direct dating methods include radiometric measurements of mineral phases from Ash 19. We provide a brief summary of these age determinations here. A more expansive assessment of these varying age data is included in the supplement to this manuscript (Supplementary Material File S1[1]).

Indirect Dates on Ash 19

Age Model Estimates. There are three types of age models that constrain the depositional age of Ash 19 (Fig. 5). Lacustrine carbonate ^{14}C data form the basis of one type. Sanidine $^{40}Ar/^{39}Ar$ data underpin a second, and a combination of the two data sets supports a third type of age model.

Age models based on ^{14}C lacustrine carbonate data suggest the following estimates for the depositional age of Ash 19: ca. 27 ka (Lajoie, 1968), ca. 40–41 ka (Benson et al., 1990), or ≥48 ka (Model 1; Kent et al., 2002). Rates of sediment deposition were assumed to be constant in each age model.

One age model that is anchored by sanidine $^{40}Ar/^{39}Ar$ data suggests that Ash 19 is no older than ca. 55 ka (Model 2; Kent et al., 2002). This model is based on the argument that the youngest age population of sanidine $^{40}Ar/^{39}Ar$ data represents the maximum age of deposition of the tephra. It also assumes that the rates of sediment deposition were constant.

[1]Supplemental Material. Assessment of Ash 19 age data; Figure S1: Measured section at the Tufa Site of Lower Wilson Creek (38.02986°N, 119.12459°W; ~1987 m); Figure S2: Our measured section of IV D of Bridgeport Creek (38.08968°N, 119.04885°W; ~2006 m); Figure S3: Measured section at the Between Site of Bridgeport Creek (38.09056°N, 119.04985°W; ~2010 m). Please visit https://doi.org/10.1130/GSAB.S.17144447 to access the supplemental material, and contact editing@geosociety.org with any questions.

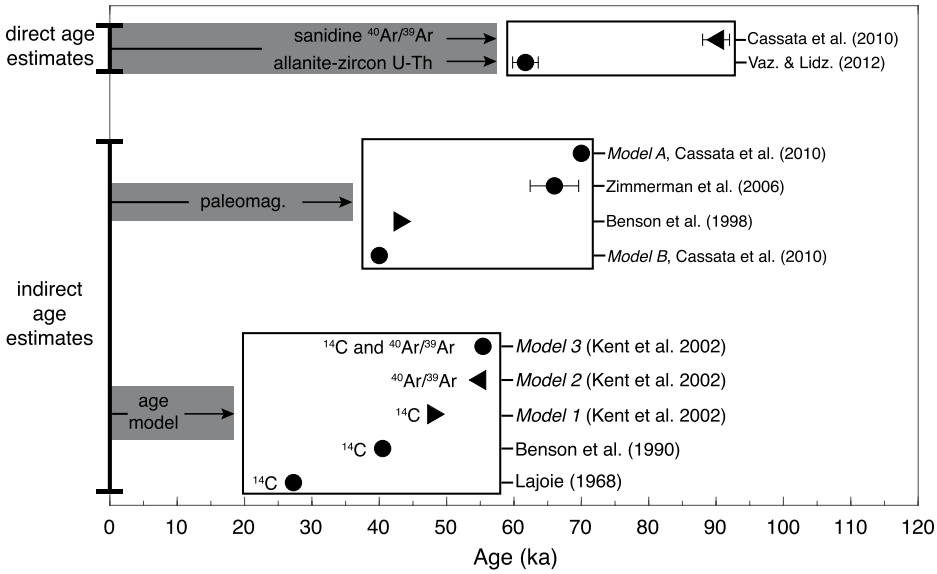

Figure 5. Direct and indirect age estimates of the depositional age of Ash 19 spanning 90–27 ka are given. Circles show age determinations. Right-pointing triangles are minimum age constraints. Left-pointing triangles are maximum age constraints. Error bars show 2-sigma uncertainties. Age model estimates based on ^{14}C dates of lacustrine macrofossils suggest that the tephra was deposited at ca. 27 ka (Lajoie, 1968), ca. 40–41 ka (Benson et al., 1990), and ≥48 ka (Model 1; Kent et al., 2002). An age model supported by sanidine ^{40}Ar/^{39}Ar data suggested a maximum age constraint of ca. 55 ka (Model 2; Kent et al., 2002). A combination of ^{14}C dates from lacustrine macrofossils and sanidine ^{40}Ar/^{39}Ar dates was used to constrain an age model that arrived at an age of 55.4 ka (Model 3, Kent et al., 2002). Interpreted paleomagnetic correlations between the Wilson Creek Formation and marine sedimentary records yield the following estimates: not younger than 43 ka (Benson et al., 1998), 66.0 ± 3.6 ka (Zimmerman et al., 2006), ca. 70 ka (Model A, Cassata et al., 2010), and ca. 41 ka (Model B, Cassata et al., 2010). Two direct age estimates offered these constraints for the deposition of Ash 19: 90.0 ± 2.0 ka via sanidine ^{40}Ar/^{39}Ar analyses (interpreted as a maximum age constraint; Cassata et al., 2010) and 61.7 ± 1.9 ka via allanite-zircon U-Th analyses (Vazquez and Lidzbarski, 2012). Note that Vaz. & Lidz. (2012) refers to Vazquez and Lidzbarski (2012).

Another age model aided by both ^{14}C lacustrine carbonate and sanidine ^{40}Ar/^{39}Ar data recommended that Ash 19 was deposited at ca. 55.4 ka (Model 3; Kent et al., 2002). This model is based on these premises: that the youngest age population of sanidine ^{40}Ar/^{39}Ar data represents the maximum age of deposition of the tephra; that the ^{14}C lacustrine carbonate data constrain the minimum age of deposition; and that the rates of sediment deposition varied.

Age Estimates Determined from Paleomagnetic Correlations. Interpreted paleomagnetic correlations between the Wilson Creek Formation and marine sedimentary records provide dissimilar (and mostly older) constraints for the depositional age of Ash 19 (Fig. 5). One interpreted correlation to two marine sedimentary records in the North Atlantic suggested that Ash 19 must be older than 43 ka (Benson et al., 1998). Attempts to correlate the Wilson Creek Formation record to GLOPIS (Global Paleointensity Stack)—a near-global stack of paleointensity time series tied to the GISP2 (Greenland Ice Sheet Project 2) age model (Laj et al., 2000, 2004)—yielded three different estimates. One is 66.0 ± 3.6 ka (Zimmerman et al., 2006). The two other age models, named Models A and B, suggested that Ash 19 was deposited at ca. 70 ka or ca. 41 ka, respectively (Cassata et al., 2010).

Direct Dates on Ash 19

There have been two efforts to directly date mineral phases of Ash 19 (Fig. 5). One is a sanidine ^{40}Ar/^{39}Ar date of 90.0 ± 2.0 ka, which the authors suggested should be interpreted as a maximum age constraint for the deposition of Ash 19 (Cassata et al., 2010). The other is an allanite-zircon U-Th date of 61.7 ± 1.9 ka (Vazquez and Lidzbarski, 2012). While the authors acknowledged that the allanite-zircon U-Th date constrained the age of magmatic crystallization, they reasoned that the date was also consistent with the eruption age based on evidence reported in other studies supporting little difference between the time of crystallization and eruption.

Carbonate U/Th Dating: Our Geochronological Approach to Dating Ash 19

In this study, we use a new geochronometer, the carbonate U/Th method, to estimate the age of Ash 19. We use this method to date carbonate deposits that underlie Ash 19, cross-cut Ash 19, and cross-cut sediments that overlie Ash 19. These data yield maximum and minimum age constraints for the deposition of the ash bed. We chose to use the U/Th method to date the carbonate samples because in cases where the initial ^{230}Th is low, the method provides highly precise and accurate ages from the present to 500 ka (Edwards et al., 1987).

METHODS

Sampling Strategy and Stratigraphic Framework

We determined the depositional age of Ash 19 in two steps. First, we used the U/Th method to date a lacustrine tufa mound that underlies the ash bed along the eastern incised wall of lower Wilson Creek (Figs. 2, 6, and S1; see footnote 1). Then we used the U/Th method to date groundwater carbonates at two sites along the eastern incised wall of Bridgeport Creek. At one of the Bridgeport Creek sites, the carbonates cross-cut lake sediments that are deposited above Ash 19 (Figs. 2, 7, and S2; see footnote 1). At the other site, the carbonate deposits cross-cut Ash 19 (Figs. 2, 8, 9, and S3; see footnote 1).

Identification of tephra beds found in our measured sections follows the stratigraphic template of the Wilson Creek Formation provided by Lajoie (1968). At the lower Wilson Creek locality, where Lajoie (1968) described the type section of the Wilson Creek Formation, tephra identification is unambiguous. However, at our sampling sites along Bridgeport Creek, tephra correlation to the type section is less certain. For example, at section IV D of Bridgeport Creek, there is only one tephra below the distinct tephra set comprising Ashes 8–15 (Lajoie, 1968). However, below this tephra set at the type section, there are four tephra: Ashes 16–19. Lajoie (1968) suggested that this discrepancy at section IV D could be resolved if the oldest unknown tephra in section IV D correlated to Ash 19.

We used a hammer and chisel to sample calcite crystals, and we documented the stratigraphic context of the samples in detail. At our lower

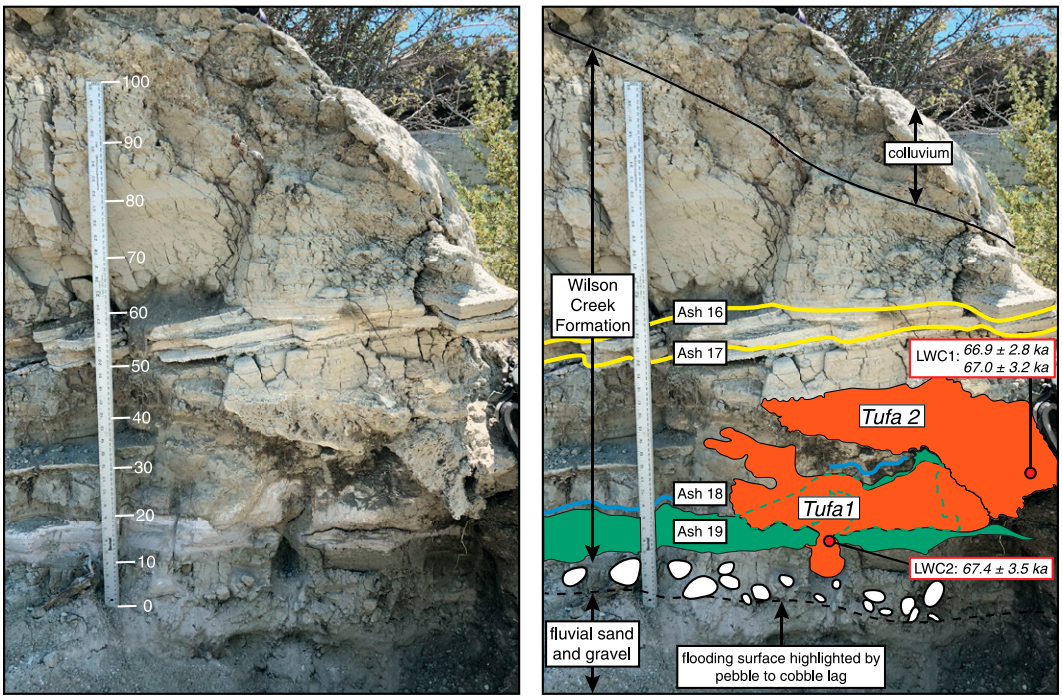

Figure 6. Photographs look to the south at the eastern wall of lower Wilson Creek at the "Tufa site." The left panel is a plain photo showing a 1-m-long rule (numbers show centimeters). The right panel shows our observations and interpretations of the stratigraphy in addition to the results of U/Th analyses made on sampled carbonates. The Tufa site shows a lake transgressive sequence comprising fluvial sand and gravel that is overlain by lacustrine silt of the Wilson Creek Formation (see labels in right panel). The sequence also contains two tufa mounds: Tufa 1 and Tufa 2. The lacustrine silt contains Ash 19 (blue-green highlight; blue-green dashed line demarcates area where the side of Tufa 1 is immediately overlain by Ash 19), Ash 18 (blue line), and Ashes 17 and 16 (yellow lines). The contact between the Wilson Creek Formation and the fluvial sand and gravel is marked by a lag bed comprising pebbles and cobbles. We interpret the base of this lag bed as a flooding surface (black dashed line). Its elevation is ~1987 m. Tufa 1 is rooted at the top of the lag bed. In addition, Tufa 1 is overlain by silt intercalated with Ashes 16–19. Tufa 2 is overlain by silt that contains Ashes 17 and 16. Our U/Th measurement on Tufa 1 (LWC2) yielded a date of 67.4 ± 3.5 ka. Our U/Th measurements on Tufa 2 (LWC1) yielded two dates: 66.9 ± 2.8 ka and 67.0 ± 3.2 ka. Since Ash 19 must be younger than Tufa 1, the tephra bed must be younger than 67.4 ± 3.5 ka. We show our measured section from this site in Figure S1 (see footnote 1).

Wilson Creek site (38.02986°N, 119.12460°W; ~1987 m; Figs. 6 and S1), the calcite crystals we selected for U/Th analysis (LWC1 and LWC2; Fig. 10) are from the porous matrix of what appears to be two lacustrine tufa mounds of unique age. We label these tufa mounds Tufa 1 and Tufa 2.

At Bridgeport Creek, we selected carbonate samples from two sites. One of these sites, IV D (38.08968°N, 119.04885°W; ~2006 m; Figs. 7 and S2) of Lajoie (1968), contains exceptionally dense carbonate deposits that outcrop above Ash 19. These deposits are underlain and overlain by lake silts, and they are packaged into four pairs of 0.5- to 1-cm-thick, thinly laminated, botryoidal, and bedding-parallel units that grew in convergent directions. For three reasons, we interpret the deposits to be subterranean groundwater mineralizations that post-date the sediments above and below. First, they are unlike the more porous structure of lacustrine tufa formed by lake and groundwater mixing (Stine, 1987). Second, they often cement the strata they are surrounded by, which is consistent with a cross-cutting relationship. Third, their laminated internal structure, botryoidal exteriors, and convergent growth habits conform to the results of lab and modeling experiments on calcite growth in confined spaces and field observations of calcite growth in syntaxial veins (Jettestuen et al., 2006; Cobbold et al., 2013; Meng et al., 2018). We sampled the oldest of the four bedding-parallel carbonate deposits (sample 1B; Figs. 7, 10, and S2), and it must be younger than Ash 19.

Our second sampling site from Bridgeport Creek is at a site upstream of Lajoie's IV D, which we call the Between site (38.09056°N, 119.04985°W; ~2010 m, Figs. 8 and S3). There we sampled dense carbonate deposits (BC1 and BC2, Figs. 9–10) that cross-cut an ash bed whose physical characteristics (e.g., color, thickness, and grain size) and depositional context are identical to those of Ash 19 at site IV D. Based on this similarity, we suggest that the two ash beds from site IV D and the Between site are correlated. Thus, the tephra at the Between site is also Ash 19, and the carbonate deposits that cross-cut it (i.e., BC1 and BC2) must be younger than Ash 19, too. The high density of the carbonates and the fact that they cross-cut the lake sediments that surround them are observations inconsistent with their origin as lacustrine tufa. Thus, we interpret them as subterranean carbonate mineralizations that formed from groundwater.

Application of the U/Th Method

We cleaned our samples by hand with tap water to remove detritus and then cleaned them by using ultrasonication in ultrapure water. We then mechanically abraded the surfaces of the carbonates using a dental drill to create a clean surface that we then drilled to liberate ~2 mg of sample powder. We chose where we liberated powder from our samples by macroscopically selecting carbonate material that showed high density and white color to avoid detrital contamination. After we dissolved and spiked the powders, we separated and chemically purified the U and Th fractions following methods presented in Chiang et al. (2019).

We measured the separated U and Th fraction solutions using a ThermoFisher Neptune Plus multicollector-inductively coupled plasma-mass spectrometer (MC-ICP-MS) at the Earth Observatory of Singapore, Nanyang Technological University, Singapore, for all samples except sample 1B, whose U and Th isotope compositions we measured at the University of Minnesota, USA, using a nearly identical laboratory procedure. We calculated ages using the ^{230}Th ($\lambda_{230} = 9.1705 \times 10^{-6}$ yr^{-1}) and ^{234}U

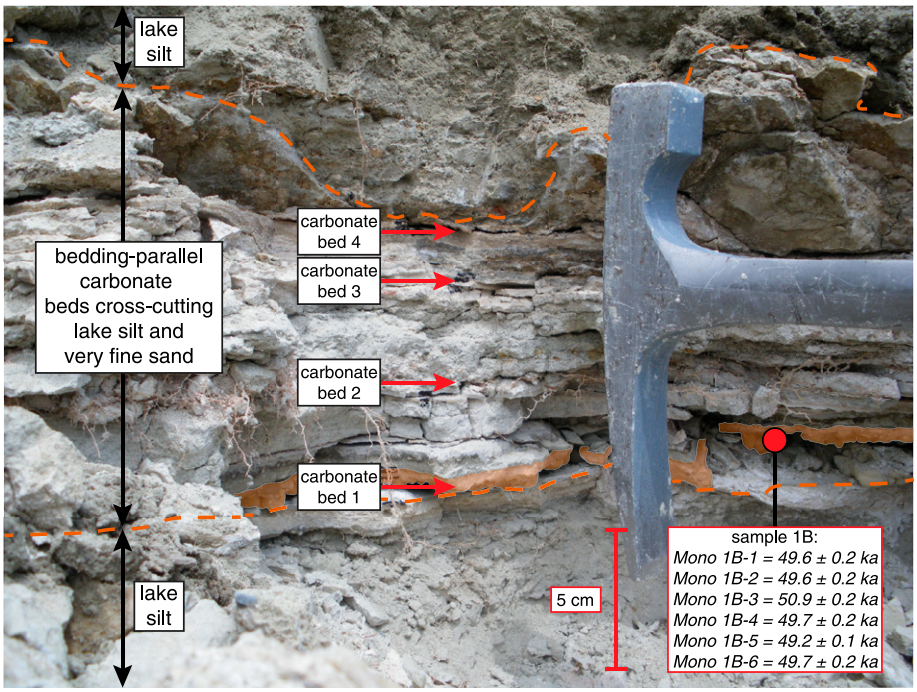

Figure 7. Photograph of the lower part of IV D of Lajoie (1968) shows bedding-parallel carbonate beds cross-cutting lacustrine silt and very fine sand. Ash 19 is ~4 cm below the bottom frame of the photo. We made six U/Th measurements on sample 1B (analyses are named Mono 1B-1 to Mono 1B-6), which we collected from the upper half of the oldest of these paired beds (highlighted in orange). The U/Th analyses resulted in five dates that spanned between ca. 49 ka and ca. 50 ka. One U/Th analysis produced an older date of ca. 51 ka. These data demonstrate that Ash 19 must be older than ca. 51 ka. We show the measured section of IV D in Figure S2 (see footnote 1).

($\lambda_{234} = 2.82206 \times 10^{-6}$ yr^{-1}) decay constants of Cheng et al. (2013) and the ^{238}U (1.55125×10^{-10} yr^{-1}) decay constant of Jaffey et al. (1971). We report the analytical uncertainties of our U/Th data at 2σ.

The initial ^{230}Th in Mono Lake water during Wilson Creek time is not known, so we use the ^{230}Th/^{232}Th atomic ratio of contemporary lake waters, with an uncertainty in the initial ratio arbitrarily assumed to be 50%, to correct for the initial ^{230}Th in our age calculation. This atomic ratio is $10 \pm 5 \times 10^{-6}$ (10 ± 5 ppm; Anderson et al., 1982). Note that samples with relatively high ^{230}Th/^{232}Th values (>1000 ppm, for instance) are less sensitive to the chosen initial correction than samples with low ^{230}Th/^{232}Th values (e.g., ~100 ppm or lower).

RESULTS OF GEOCHRONOLOGY

Carbonate U/Th data are presented in Table 1, and the context and U/Th dating results of the samples are shown in Figures 6–10 and S1–S3 and diagrammed in Figure 11.

Carbonate samples from lower Wilson Creek (Figs. 6 and 10) have a high thorium content. The ^{232}Th concentrations are ~250–490 ppb, and the ^{238}U/^{232}Th ratios are between 12 and 15. These high thorium values make the uncertainty in the initial ^{230}Th correction relatively large, which yields age uncertainties that are ~4–5%. One analysis of sample LWC2 from Tufa 1 yielded

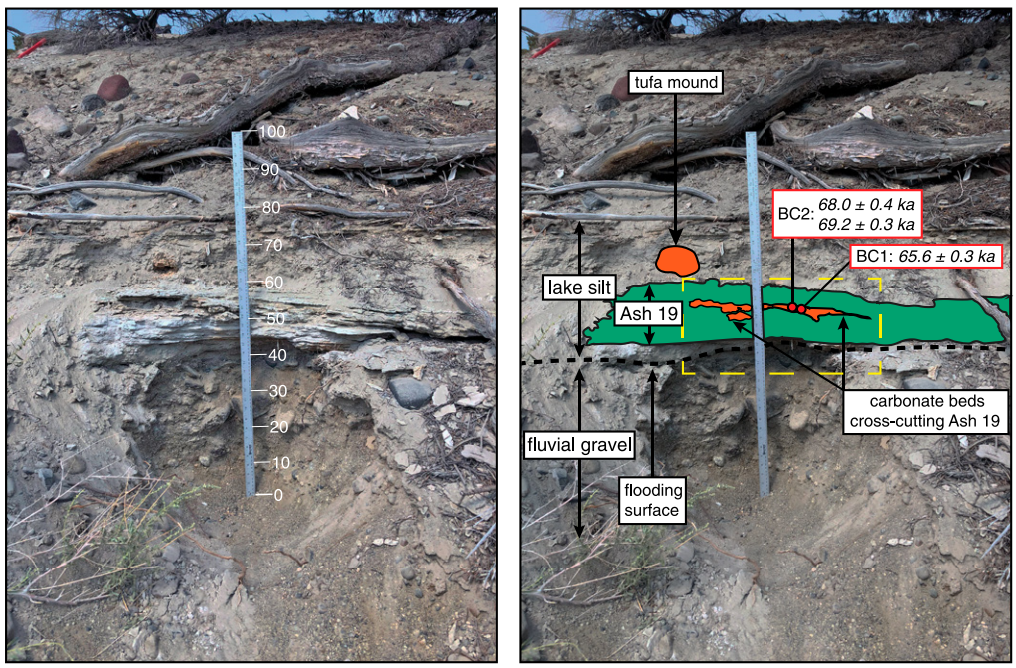

Figure 8. Photographs look toward the eastern canyon wall of Bridgeport Creek at our "Between site." The left panel is a plain photo showing a 1-m-long rule (numbers show centimeters). The right panel highlights the sequence of sediments at the site, which we interpret to represent a lake transgressive sequence. This sequence shows fluvial gravel overlain by lacustrine silt that is intercalated with Ash 19 (green highlight). The contact between the fluvial gravel and lacustrine silt is a flooding surface (black dashed line). Ash 19 is cross-cut by thin carbonate beds (orange highlight). Two samples (BC1 and BC2) collected from one of the thin carbonate beds (orange highlight) that cross-cut Ash 19 yielded three U/Th dates of 65.6 ± 0.3 ka (BC1), 68.0 ± 0.4 ka (BC2), and 69.2 ± 0.3 ka (BC2). These dates are minimum age constraints for the deposition of Ash 19 and the underlying flooding surface. Our measured section from this site is shown in Figure S3 (see footnote 1). Yellow dashed box shows location encompassing Figure 9.

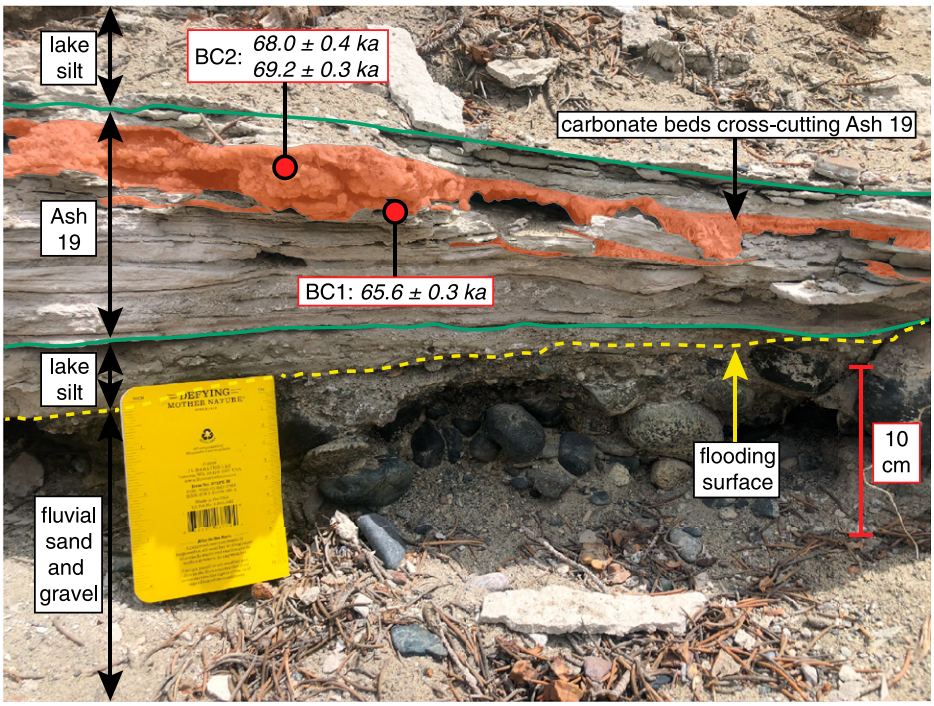

Figure 9. Photograph shows the eastern canyon wall of Bridgeport Creek at our "Between site" (see area highlighted by yellow dashed line in Fig. 8 for spatial context). Our observations reported in our measured section from this site (Fig. S3; see footnote 1) support the interpretation that the contact between the lacustrine silt and fluvial gravel represents a flooding surface (yellow dashed line). Ash 19, whose top and bottom we mark with a green line, is deposited 2 cm above the flooding surface. We collected two samples (BC1 and BC2) from one of the thin carbonate beds (orange highlight) that cross-cuts Ash 19. BC1 yielded a U/Th date of 65.6 ± 0.3 ka. BC2 yielded U/Th dates of 68.0 ± 0.4 ka and 69.2 ± 0.3 ka. These dates are minimum age constraints for the deposition of Ash 19 and the underlying flooding surface.

an age of 67.4 ± 3.5 ka. Since Tufa 1 is overlain by Ash 19, a date on LWC2 provides a maximum constraint on the age of Ash 19. Two analyses of sample LWC1 from Tufa 2 yielded ages of 66.9 ± 2.8 ka and 67.0 ± 3.2 ka. Because we found the three-dimensional exposure of the section insufficient to confidently interpret how Tufa 2 relates to the stratigraphic position of Tufa 1 or Ashes 18 and 19, we offer the most conservative interpretation of the dates on LWC1 of Tufa 2: that they provide a maximum age constraint on Ash 17.

Carbonate samples from Bridgeport Creek have much lower thorium contents; ^{232}Th concentrations are ~1–34 ppb, and ^{238}U/^{232}Th ratios are 171–3536. These lower thorium values introduce less uncertainty on the initial ^{230}Th correction, which results in age uncertainties that are between ~0.3% and 0.5%. Six measurements of sample 1B from IV D of Lajoie (1968) produced ages between 49.2 ± 0.1 and 50.9 ± 0.2 ka (Figs. 7 and 10). One measurement of sample BC1 from our Between site produced an age of 65.6 ± 0.3 ka (Figs. 8–10). Two measurements of sample BC2 from our Between site resulted in older ages of 68.0 ± 0.4 ka and 69.2 ± 0.3 ka (Figs. 8–10). All of the dates from IV D and the Between site provide minimum age constraints for the deposition of Ash 19.

DISCUSSION

Geochronology

Our strongest interpretation of the depositional age of Ash 19 comes from the minimum age constraint that is established by the oldest low-thorium sample that cross-cuts Ash 19 at the Between site of Bridgeport Creek. U/Th analyses of carbonates from this site have ^{230}Th/^{232}Th atomic ratios that range between ~1800 ppm and 24,700 ppm. Such high ratios mean that the age correction is insensitive to uncertainties incurred by our assumptions about the initial ^{230}Th/^{232}Th ratios. Thus, we can be confident that Ash 19 must be older than 69.2 ± 0.3 ka.

A 69.2 ± 0.3 ka minimum age for Ash 19 is consistent with the six U/Th dates that we measured from sample 1B of IV D, which is younger than Ash 19. The six dates span 49.2 ± 0.1 ka to 50.9 ± 0.2 ka and show relatively high ^{230}Th/^{232}Th atomic ratios (~9400–42,600 ppm), which underscores the fact that the age correction of these measurements is insensitive to the uncertainties regarding our chosen initial ^{230}Th/^{232}Th ratio. While these data show that Ash 19 must be older than 50.9 ± 0.2 ka, the older age constraint of 69.2 ± 0.3 ka from the Between site affords the most useful minimum age constraint for the deposition of Ash 19.

Our best maximum age constraint for Ash 19 derives from sample LWC2 of Tufa 1. The corrected age of LWC2 is more sensitive to the chosen initial ratio than the samples from Bridgeport Creek because of the relatively lower ^{230}Th/^{232}Th atomic ratio of LWC2 (~100 ppm). If we use our preferred initial ^{230}Th/^{232}Th correction value of 10 ppm, the determined age of the sample is 67.4 ± 3.5 ka. If we, on the other hand, correct the age using a less conservative initial value that assumes the amount of radiogenically ingrown ^{230}Th in the sample is higher, the corrected age will be older and have a lower uncertainty. For example, if the chosen initial ^{230}Th/^{232}Th reflects the bulk earth ratio of 4.4 ppm (Richards and Dorale, 2003), we arrive at a date of 70.2 ± 1.6 ka. While Ash 19 cannot be older than this date, we suggest that it is not a tenable maximum age constraint because it likely underestimates the initial ^{230}Th/^{232}Th correction. Thus, in the discussion herein, we refer to the more reasonable estimate of 67.4 ± 3.5 ka as our maximum age constraint for the deposition of Ash 19.

In spite of the nominal difference between our maximum and minimum age constraints for the deposition of Ash 19 (67.4 ± 3.5 ka versus 69.2 ± 0.3 ka, respectively), the two dates agree. This agreement leads us to consider it highly likely that the age of Ash 19 is very close to the 69.2 ± 0.3 ka minimum age of sample BC2 from Bridgeport Creek.

Two implications emerge from our 69.2 ± 0.3 ka constraint on the minimum depositional age of Ash 19. One is that it provides an independent, absolute date that constrains the basal age of the Wilson Creek Formation. The second is how the date approximates the start of the most recent wet interval in the Mono Basin.

Assessment of Previous Geochronologic Data within the Context of Our New Carbonate U/Th Data

We group the age interpretations of Ash 19 into two groups: one that is younger than 43 ka and one that is older than 43 ka (Fig. 12). Our high-precision minimum age constraint of 69.2 ± 0.3 ka contradicts the age estimates of the younger group, which includes the ca. 27 ka model age of Lajoie (1968) and the ca. 40–41

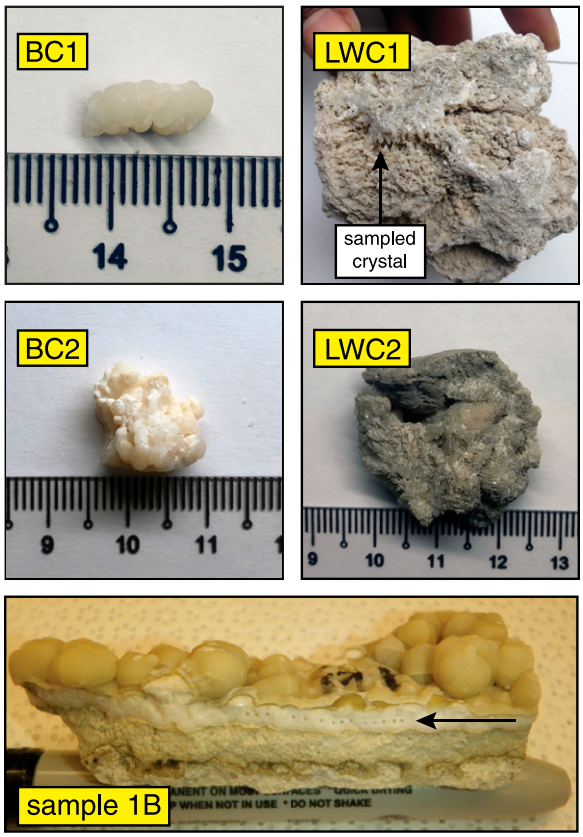

Figure 10. Photographs show carbonate samples we dated using the U/Th method. Analyses on samples from the Between site of Bridgeport Creek yielded a date of 65.6 ± 0.3 ka on BC1 and dates of 68.0 ± 0.4 ka and 69.2 ± 0.3 ka on BC2. Analyses on samples from the Tufa sites yielded two dates of 66.9 ± 2.8 ka and 67.0 ± 3.2 ka on LWC1 and a date of 67.4 ± 3.5 on LWC2. Six analyses on "sample 1B" from section IV D of Bridgeport Creek produced these dates: 49.6 ± 0.2 ka, 49.6 ± 0.2 ka, 50.9 ± 0.2 ka, 49.7 ± 0.2 ka, 49.2 ± 0.1 ka, and 49.7 ± 0.2 ka. Arrows point to sites that were powdered for U/Th analysis. Rule shows centimeters. "Sample 1B" is ~8.5 cm long. LWC1 is ~7.5 cm long.

ka model age of Benson et al. (1990). Within the older group, our ~69 ka age determination agrees with the 66.0 ± 3.6 ka estimate put forward in Zimmerman et al. (2006), the 70 ka age inferred from Model A of Cassata et al. (2010), and the 90.0 ± 2.0 ka sanidine $^{40}Ar/^{39}Ar$ maximum age estimate of Cassata et al. (2010). Our age determination also agrees with the >43 ka interpretation of Benson et al. (1998) and the ≥48 ka interpretation of Model 1 reported in Kent et al. (2002). This agreement lends support to the contention that the ^{14}C ages of Wilson Creek Formation lacustrine carbonates are best interpreted as minimum depositional ages because they are anomalously young owing to post-depositional carbon addition (Kent et al., 2002; Hajdas et al., 2004; Zimmerman et al., 2006). This contention is also corroborated by evidence reported in Zimmerman et al. (2012) that shows the potential for contamination of Mono Basin lacustrine carbonates to exceed 10% modern carbon.

Within the ages contained in the older group, we argue that the following estimates are too young: the ca. 55 ka maximum age constraint shown in Model 2 of Kent et al. (2002) and the 61.7 ± 1.9 ka date derived from allanite-zircon U-Th data of Vazquez and Lidzbarski (2012). We argue that the 14 k.y. disparity between our estimate and the ca. 55 ka maximum age constraint of Model 2 can be explained if the minimum age population of the $^{40}Ar/^{39}Ar$ ages that supported the model interpretation is either too young or the authors' assumption of constant rates of sedimentation deposition is invalid.

The >5 k.y. discordance between our newly reported carbonate U/Th date and the 61.7 ± 1.9 ka allanite-zircon U-Th date (Vazquez and Lidzbarski, 2012) is enigmatic and will require further study. We find no fault with the analytical data from Vazquez and Lidzbarski (2012). While discordance between carbonate U/Th and allanite-zircon U-Th ages can exist, such disagreement is opposite to what could be explained by the difference between eruption and crystallization ages; that is, allanite-zircon U-Th ages may be equal to or older than the eruption or depositional age of Ash 19. We speculate that the discordance could be resolved if Vazquez and Lidzbarski (2012) sampled a tephra layer at the South Shore locality that is distinct from Ash 19 at the type locality. We have taken this scenario into consideration because the stratigraphy at the South Shore site is complex. Lajoie (1968) showed that the strata below Ash 17 at the South Shore site are folded and contorted, which leads to uncertainty in identifying the ash beds below Ash 17 in this part of the basin.

The Onset of Wetness in the Mono Basin Correlates with the Last Glacial Inception

The Wilson Creek Formation of the Mono Basin correlates with an interval of heightened wetness whose beginning corresponds to the deposition of Ash 19. Our carbonate U/Th data constrain the depositional age of the tephra and the onset of a wetter Mono Basin to be equal to or close to 69.2 ± 0.3 ka. The timing of this hydroclimatic shift in the Mono Basin agrees with the timing of similar changes observed in other records of hydroclimate from the Basin and Range. The best example of this agreement is shown by the correspondence between the shift to wetness in the Mono Basin and a rise in the water table of the caves of Devils Hole, southwestern Nevada (Szabo et al., 1994; Wendt et al., 2018; Figs. 1 and 13C). In addition, it agrees with a cooling of the deep sea and/or growth of continental ice sheet volume (Fig. 13A; Lisiecki and Raymo, 2005), a rapid drawdown of atmospheric CO_2 (Fig. 13B; Bereiter et al., 2012; Menking et al., 2019; Menking, 2019), and a minimum in Northern Hemisphere summer insolation (Fig. 13D; Berger and Loutre, 1991). These hydrospheric, cryospheric, and atmospheric changes correlate with the last glacial inception, which is marked by the boundary between Marine Isotope Stages (MIS) 5 and 4 (Fig. 13). This is the boundary between the last interglaciation, MIS 5, and the first of three marine isotope stages that compose the Last Glaciation—MIS 4 (ca. 71–57 ka), 3 (ca. 57–29 ka), and 2 (ca. 29–14 ka) (Lisiecki and Raymo, 2005).

A Turn to Wetness across the Basin and Range at the MIS 5/4 Boundary

The longest and most precisely dated record of regional hydroclimatic change is derived from carbonates of the Devils Hole caves (Figs. 1 and 13C; Szabo et al., 1994; Wendt et al., 2018). Devils Hole is the site of one of the earliest U/Th-dated records of hydroclimate derived from speleothems (Winograd et al., 1988), and it is a site that has since fostered a long history of paleohydroclimatic study (e.g., Winograd et al., 1992; Imbrie et al., 1993; Winograd et al., 2006; Moseley et al., 2016). A recent study of Devils Hole shows a rapid water table rise that is correlated with the MIS 5/4 boundary (Fig. 13C; Wendt et al., 2018). The water table rise began between 78.9 ± 0.4 ka and 74.4 ± 0.4 ka and continued until sometime after 69.2 ± 0.3 ka. The similarity of these data to the ca. 69 ka rise of Mono Lake lends support to the interpretation that there was a regionally coherent pivot toward wetter conditions sometime in the interval of ca. 79–69 ka. However, the data also

TABLE 1. U/Th DATING RESULTS

Location (CSRS Epoch 2017.50, NAD83) Sample number	Description	^{238}U (ppb)	^{232}Th (ppb)	^{238}U/^{232}Th	^{230}Th/^{232}Th (atomic ratio, $\times 10^{-6}$)	δ^{234}U* (measured, ‰)	^{230}Th/^{238}U (activity)	^{230}Th age (yr) (uncorrected)	^{230}Th age (yr) (corrected)	$\delta^{234}U_{initial}$ ** (corrected, ‰)	^{230}Th age (yr B.P.)*** (corrected)	Report ages (yr B.P.)
Tufa site, lower Wilson Creek (38.02986°N, 119.12460°W)												
LWC1	lacustrine carbonate	7324 ± 10	487.3 ± 9.8	15.0 ± 0.3	134 ± 3	121 ± 2	0.5410 ± 0.0012	70859 ± 312	**66952 ± 2783**	146 ± 3	**66887 ± 2783**	**66900 ± 2800**
LWC1	lacustrine carbonate	3254 ± 5	251.0 ± 5.0	13.0 ± 0.3	116 ± 2	118 ± 2	0.5437 ± 0.0012	71597 ± 329	**67042 ± 3242**	143 ± 3	**66977 ± 3242**	**67000 ± 3200**
LWC2 (3a)	lacustrine carbonate	5276 ± 11	440.6 ± 8.9	12.0 ± 0.2	108 ± 2	120 ± 2	0.5487 ± 0.0017	72378 ± 355	**67447 ± 3509**	145 ± 3	**67379 ± 3509**	**67400 ± 3500**
Site IV D, Bridgeport Creek (38.08968°N, 119.04885°W)												
Mono 1B-1	groundwater carbonate	20722 ± 29	5.9 ± 0.3	3536 ± 160	42563 ± 1926	933 ± 2	0.7301 ± 0.0015	49659 ± 151	**49650 ± 151**	1073 ± 3	**49590 ± 151**	**49590 ± 150**
Mono 1B-2	groundwater carbonate	17292 ± 28	7.2 ± 0.1	2404 ± 40	28848 ± 480	926 ± 2	0.7278 ± 0.0021	49691 ± 187	**49677 ± 188**	1065 ± 2	**49617 ± 188**	**49620 ± 190**
Mono 1B-3	groundwater carbonate	18931 ± 34	9.2 ± 0.1	2065 ± 33	25438 ± 407	937 ± 2	0.7472 ± 0.0021	50928 ± 191	**50912 ± 191**	1082 ± 2	**50852 ± 191**	**50850 ± 190**
Mono 1B-4	groundwater carbonate	17736 ± 29	11.6 ± 0.2	1531 ± 31	18421 ± 374	928 ± 2	0.7298 ± 0.0017	49779 ± 160	**49758 ± 161**	1068 ± 2	**49698 ± 161**	**49700 ± 160**
Mono 1B-5	groundwater carbonate	10272 ± 15	6.9 ± 0.1	1496 ± 30	17761 ± 361	918 ± 2	0.7200 ± 0.0016	49281 ± 144	**49259 ± 144**	1055 ± 2	**49199 ± 144**	**49200 ± 140**
Mono 1B-6	groundwater carbonate	9821 ± 17	12.4 ± 0.3	792 ± 16	9420 ± 192	908 ± 2	0.7218 ± 0.0018	49781 ± 165	**49740 ± 167**	1044 ± 2	**49680 ± 167**	**49680 ± 170**
Between site, Bridgeport Creek (38.09056°N, 119.04985°W)												
BC1	groundwater carbonate	2637 ± 4	1.06 ± 0.03	2477 ± 61	24692 ± 610	308 ± 2	0.6046 ± 0.0013	65718 ± 245	**65699 ± 245**	371 ± 3	**65633 ± 245**	**65630 ± 250**
BC2	groundwater carbonate	5793 ± 12	33.9 ± 0.7	171 ± 3	1832 ± 37	365 ± 2	0.6512 ± 0.0018	68316 ± 297	**68047 ± 351**	443 ± 3	**67979 ± 351**	**67980 ± 350**
BC2	groundwater carbonate	3978 ± 6	9.1 ± 0.2	438 ± 9	4710 ± 99	353 ± 2	0.6525 ± 0.002	69411 ± 295	**69305 ± 303**	429 ± 2	**69237 ± 303**	**69240 ± 300**

Note: U decay constants are $\lambda_{238} = 1.55125 \times 10^{-10}$ (Jaffey et al., 1971) and $\lambda_{234} = 2.82206 \times 10^{-6}$ (Cheng et al., 2013). Th decay constant is $\lambda_{230} = 9.1705 \times 10^{-6}$ (Cheng et al., 2013). ppb—parts per billion.

*$\delta^{234}U = ([^{234}U/^{238}U]_{activity} - 1) \times 1000‰$, where ‰ stands for per mil.

**$\delta^{234}U_{initial}$ was calculated based on ^{230}Th age (T), i.e., $\delta^{234}U_{initial} = \delta^{234}U_{measured} \times e^{\lambda 234 \times T}$.

***B.P. stands for "Before Present" where the "Present" is defined as the year 1950 A.D. Corrected ^{230}Th ages assume the initial ^{230}Th/^{232}Th atomic ratio is $10 \pm 5 \times 10^{-6}$. The error on the initial value is arbitrarily assumed to be 50%.

afford an alternative interpretation: that the transition to wetter conditions in the Mono Basin occurred 5–10 k.y. after the transition took place in the watershed of Devils Hole. We suggest that the apparent lag can be reconciled in two ways. The lag can be reconciled if, between 78.9 ± 0.4 ka and 74.4 ± 0.4 ka, the level of Mono Lake began to rise but stayed below that of our lowest elevation site (~1987 m) until ca. 69 ka. The lag also can be reconciled if lacustrine strata deposited as early as ca. 79 ka and as late as ca. 69 ka are eroded from our sites. If this second scenario is true, the erosion of such strata would have occurred if Mono Lake fluctuated between elevations that were below and above those of our sites (~1987–2010 m). A lake fall would have coincided with fluvial incision and subaerial erosion. A lake rise, on the other hand, would have caused shoreface erosion by wave action. While there is no limit to the number of times these erosional events could have occurred between 79 ka and 69 ka, the final event must have coincided with the ca. 69 ka rise of the lake. To test the validity of these two scenarios, we need to observe sedimentary sequences that include Wilson Creek Formation and pre-Wilson Creek Formation strata in a continuous sequence. Such strata are not known to be extensively exposed above the current lake level (Lajoie, 1968). Thus, the recovery and dating of sediments that extend through and below the Wilson Creek Formation sequence by coring in the lake will be necessary to resolve the uncertainty.

While other hydroclimatic records from the Basin and Range are not dated as precisely as those at Devils Hole, they also show evidence of a pivot to wetter hydroclimate in near harmony with what we observed in the Mono Basin. For example, sediment geochemical data from Owens Lake (e.g., $CaCO_3$ content), which are shown to closely resemble the pattern of changes recorded in marine $\delta^{18}O$ stacks over the past 500 k.y., indicate wetter hydroclimate during the time spanning 74–65 ka (Bischoff et al., 1997; Menking et al., 1997). Exposure ages of shorelines from lakes in western Nevada are consistent with expansive lakes during MIS 4 (Kurth et al., 2011). Tufa U/Th ages suggest a switch from relatively dry to relatively wet conditions in the Pyramid Lake sub-basin of Lake Lahontan at ca. 60 ka (Szabo et al., 1996). In addition, stratigraphic observations from the Bonneville Basin support the interpretation that wetter conditions existed there sometime between 80 ka and 40 ka (Oviatt et al., 1987), and another study suggests that these wetter conditions are dated to 59.0 ± 5.0 ka (Kaufman et al., 2001). Limnological data from the Summer Lake Basin support the interpretation of increased wetness

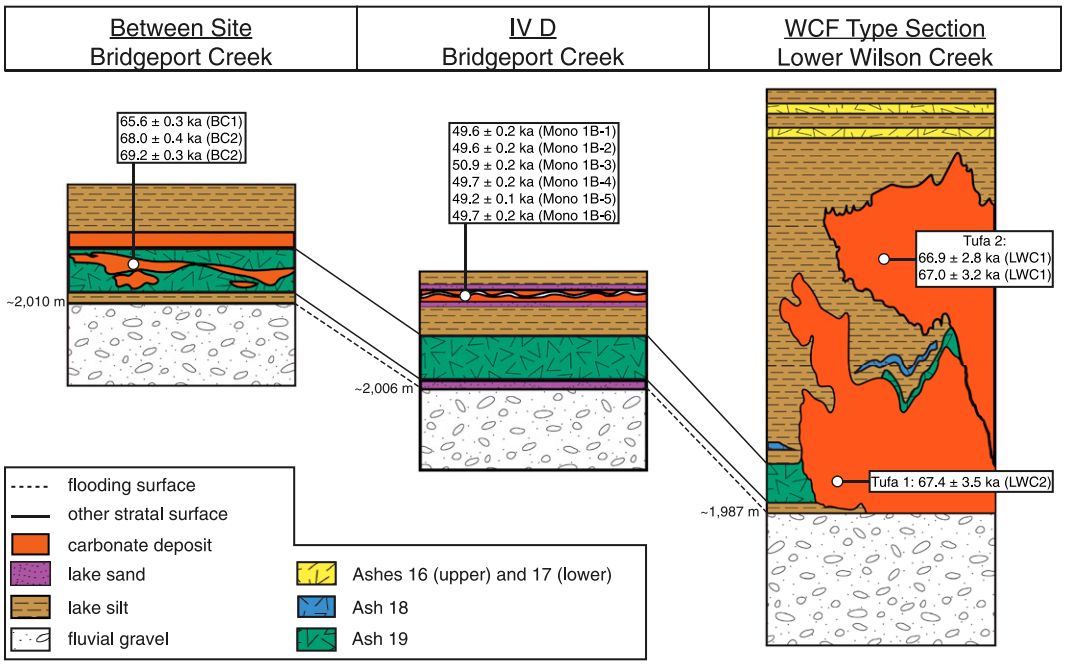

Figure 11. Summary diagram shows stratigraphic correlation between the three sites—Between site, IV D, and Tufa site—where we sampled and dated carbonates that were either younger or older than Ash 19. Carbonate deposits from IV D and the Between site postdate the deposition of Ash 19. The oldest U/Th date we measured from the carbonates from IV D and the Between site is 69.2 ± 0.3 ka (sample BC2), which suggests that Ash 19 was deposited before this date. At the Tufa site, the lacustrine tufa mound we called Tufa 1 is overlain by Ash 19. Thus, Tufa 1 is older than the ash bed. Our U/Th analysis of Tufa 1 (sample LWC2) suggested that Tufa 1 is 67.4 ± 3.5 ka, which makes Ash 19 younger than this date. These U/Th data show that Ash 19 was deposited before 69.2 ± 0.3 ka but after 67.4 ± 3.5 ka.

in south-central Oregon at ca. 89–50 ka (Cohen et al., 2000). In addition, travertine deposition at 69 ± 3 ka and 61 ± 10 ka in northern Arizona points to a time of wetter than present conditions in the southwestern U.S. (Szabo, 1990). Thus, within the chronologic uncertainties of these records, all are consistent with a regional shift to wetter conditions at ca. 70 ka.

The Beginning of Wetness in the Mono Basin in the Context of Global Paleoclimatic Records

Paleoclimatic observations dispersed across the planet reveal monumental atmospheric, cryospheric, and hydrospheric changes at the MIS 5/4 boundary (Fig. 13). One conspicuous example is a 40 ppm decline of atmospheric CO_2 documented between ca. 72 ka and ca. 67 ka that amounts to ~40% of the last glacial-interglacial CO_2 variability (Fig. 13B; Bereiter et al., 2012; Schneider et al., 2013; Ahn and Brook, 2014; Marcott et al., 2014; Menking et al., 2019; Menking, 2019). Also approximately synchronous is an abrupt cooling of North and South Atlantic surface waters (Bond

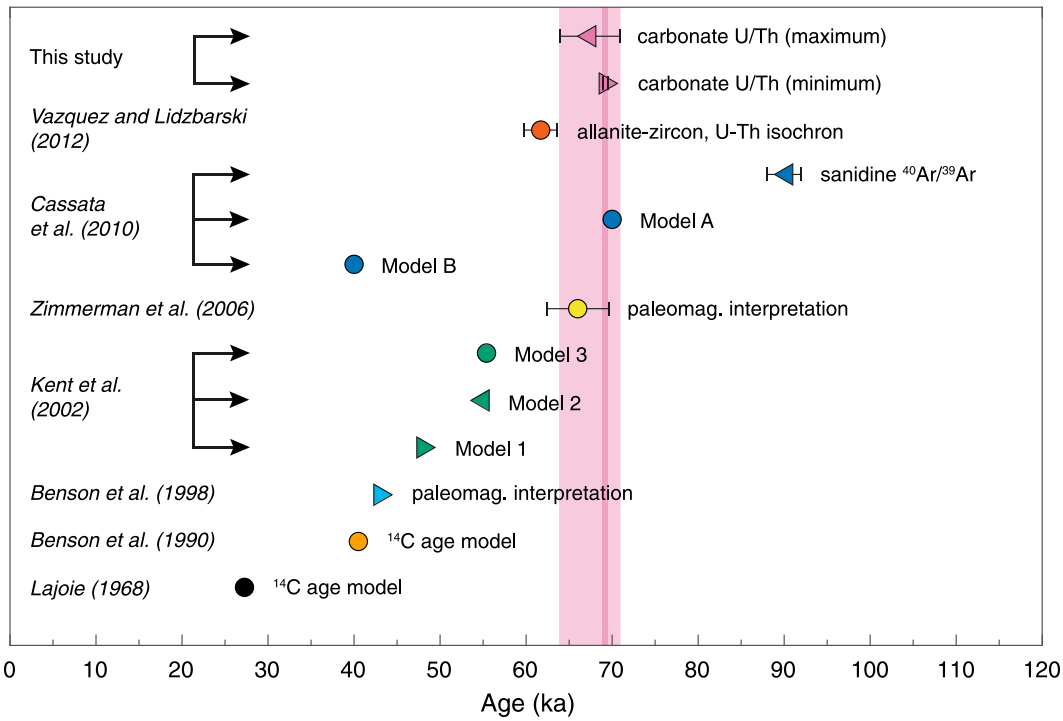

Figure 12. Compilation diagram shows geochronologic estimates of the age of Ash 19. Circles show age determinations. Right-pointing triangles are minimum age constraints. Left-pointing triangles are maximum age constraints. Error bars show 2-sigma uncertainties. Pink vertical bars represent the time spanning the age uncertainty of our carbonate U/Th age determinations. The wider of the two vertical bars shows 3.5 k.y. uncertainty on the 67.4 ka nominal age of the maximum estimate. The narrower vertical bar shows 0.3 k.y. uncertainty on 69.2 ka nominal age of minimum estimate. Paleomag.—paleomagnetic.

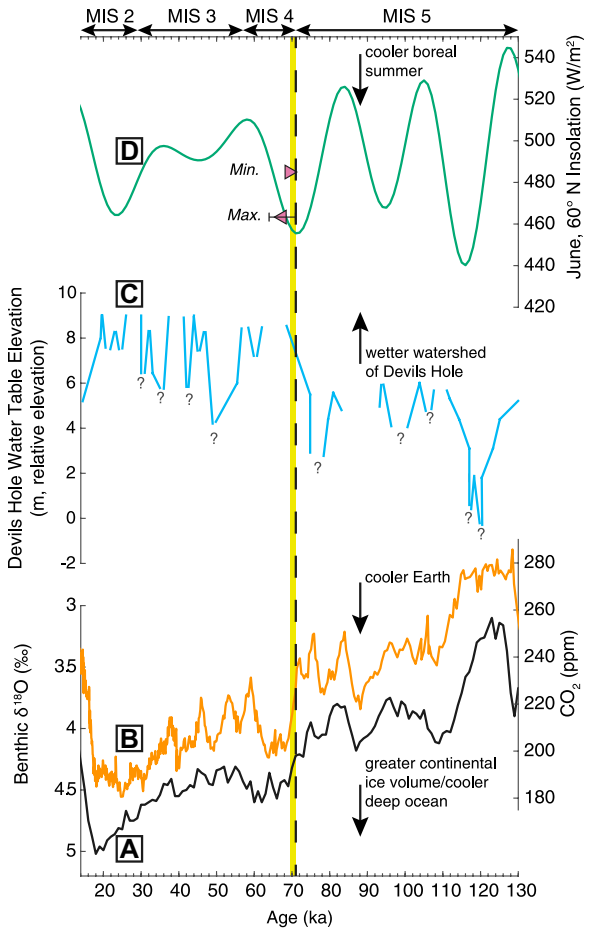

Figure 13. Shown from bottom to top: (A) global stack of marine benthic $\delta^{18}O$ time series, black time series (Lisiecki and Raymo, 2005), and their interpreted divisions, termed Marine Isotope Stages (MIS; time spanning each stage is shown with double-headed arrows at top of figure); (B) compilation of Bereiter et al. (2015) that shows atmospheric carbon dioxide data from Antarctic ice core records, orange time series (compilation also includes data from these studies: Bereiter et al., 2012; Schneider et al., 2013; Ahn and Brook, 2014; Marcott et al., 2014); (C) water table fluctuation record of Devils Hole, light-blue time series (Szabo et al., 1994; Wendt et al., 2018); (D) summer insolation at 60° N, blue-green time series (Berger and Loutre, 1991). The yellow vertical bar represents the interval that spans the following combined time: that which is younger than our maximum age constraint for Ash 19 (left-pointing, pink triangle with 2-sigma error bar) and that which is older than our minimum age constraint for Ash 19 (right-pointing, pink triangle; 2-sigma error is not shown since it is smaller than the datum marker). Thus, the yellow vertical bar shows the probable interval during which wetter hydroclimate initiated in the Mono Basin. Note the similarity in timing between the shift to wetter conditions in the Mono Basin and climatic changes inferred from the other paleoclimatic time series at the inception of the Last Glaciation at ca. 70 ka (MIS 5/4 boundary; vertical, black dashed line). The top axis shows age (ka), and its scaling mirrors the bottom axis.

et al., 1993; Barker and Diz, 2014), a reordering of the ocean's thermohaline circulation (e.g., Piotrowski et al., 2005), a southward shift of the thermal equator and weakening of the Asian monsoon (Wang, 2001; Wang et al., 2008; Deplazes et al., 2013; Cai et al., 2015), and an expansion of mountain glaciers and continental ice sheets (Vincent and Prest, 1987; Stokes et al., 2012; Kleman et al., 2013; Schaefer et al., 2015; Seguinot et al., 2016; Batchelor et al., 2019; Doughty et al., 2021; Peltier et al., 2021). These changes in the atmosphere and hydrosphere were coeval with a minimum in Northern Hemisphere summer insolation (Fig. 13D; Berger and Loutre, 1991). The study presented here makes clear that the onset of wet conditions in the Mono Basin at ca. 70 ka corresponds to the global climatic rearrangement that happened when the planet last transitioned from an interglacial to a glacial state.

Potential Causal Underpinnings of Regional Wetness during MIS 4

Results from recent modeling efforts that explored how MIS 4 boundary conditions impacted Northern Hemisphere hydroclimate are consistent with greater precipitation and reduced summer temperatures across the Basin and Range compared to those of the preceding and present interglacials (Löfverström et al., 2014; Tulenko et al., 2020). The cause of this precipitation increase was suggested to reflect a strengthening of the midlatitude westerlies. The simulated strengthening of the westerlies was linked to the greater temperature gradient in the Northern Hemisphere between the pole and equator during MIS 4, which itself reflected the orbital forcing of the time and the impact to surface albedo of the more expansive footprints of boreal ice sheets (and, in particular, the North American ice sheets). We infer that these simulated changes in precipitation and summer temperatures during the transition from MIS 5–4 would have shifted the regional water balance in favor of increased wetness and caused Mono Lake to expand at ca. 70 ka.

Implications for the Eruptive History of the Mono Craters

Our ca. 70 ka age estimate for the deposition of Ash 19 yields a new timestamp for one of the earliest known eruptions of the Mono Craters (Marcaida et al., 2019). This new timestamp lengthens the record of explosive rhyolitic activity from the Mono Craters system by a few thousand years (Marcaida et al., 2019). It also suggests the need for additional constraints across the basin of the oldest tephra layers associated with the Mono Craters and other regional silicic centers (e.g., Bevilacqua et al., 2018). Such data may help to document the style and frequency of volcanic eruptions impacting the basin. Furthermore, those tephra deposits are important time markers across the western U.S.

CONCLUSION

Using the U/Th disequilibrium dating method to date lacustrine and groundwater carbonates in association with Ash 19 of the Wilson Creek Formation, we constrain the depositional age of the tephra to be no younger than 69.2 ± 0.3 ka and no older than 67.4 ± 3.5 ka; it is likely close to 69 ka. These constraints show that the beginning of the most recent interval of persistent wetness in the Mono Basin correlates with the inception of the Last Glaciation at the start of MIS 4. This temporal correlation supports studies that point to the impact of glacial climate conditions on enhancing wetness across the Basin and Range. Furthermore, based on this correlation and on similar evidence throughout the region, we hypothesize that other hydrologically closed lakes of the Basin and Range expanded at the inception of glacial conditions at ca. 70 ka.

ACKNOWLEDGMENTS

This research was supported by the Gary Comer Science and Education Foundation and the Lamont-Doherty Earth Observatory Climate Center. Financial support from the Ford Foundation aided in the writing of this manuscript. We are grateful to the Mono Lake Committee and Shirin and Steve Connett for years of field and technical support that were instrumental in making this work a success. We thank P. Adamek for help and guidance on the writing of the manuscript.

R. L. Edwards kindly provided access to the lab facility for U/Th dating during the early stage of this study. X.W. acknowledges support from the Singapore Ministry of Education (grant nos. MOE2019-T2-1-1744 and RG13/20) and the Earth Observatory of Singapore. This is LLNL-JRNL-817260 and comprises EOS contribution number 376.

REFERENCES CITED

Adams, K.D., and Rhodes, E.J., 2019, Late Pleistocene to present lake-level fluctuations at Pyramid and Winnemucca lakes, Nevada, USA: Quaternary Research, v. 92, p. 146–164, https://doi.org/10.1017/qua.2018.134.

Ahn, J., and Brook, E.J., 2014, Siple Dome ice reveals two modes of millennial CO_2 change during the last ice age: Nature Communications, v. 5, p. 1–6, https://doi.org/10.1038/ncomms4723.

Anderson, R.F., Bacon, M.P., and Brewer, P.G., 1982, Elevated concentrations of actinides in Mono Lake: Science, v. 216, p. 514–516, https://doi.org/10.1126/science.216.4545.514.

Antevs, E., 1952, Climatic history and the antiquity of man in California: University of California Archaeological Survey Reports, v. 16, no. 16, p. 23–31.

Bailey, R.A., 2004, Eruptive history and chemical evolution of the precaldera and postcaldera basalt-dacite sequences, Long Valley, California: Implications for magma sources, current magmatic unrest, and future volcanism: U.S. Geological Survey Professional Paper, 75 p.

Barker, S., and Diz, P., 2014, Timing of the descent into the last Ice Age determined by the bipolar seesaw: Paleoceanography, v. 29, p. 489–507, https://doi.org/10.1002/2014PA002623.

Batchelor, C.L., Margold, M., Krapp, M., Murton, D.K., Dalton, A.S., Gibbard, P.L., Stokes, C.R., Murton, J.B., and Manica, A., 2019, The configuration of Northern Hemisphere ice sheets through the Quaternary: Nature Communications, v. 10, no. 3713, https://doi.org/10.1038/s41467-019-11601-2.

Benson, L.V., and Paillet, F.L., 1989, The use of total lake-surface area as an indicator of climatic change: Examples from the Lahontan Basin: Quaternary Research, v. 32, p. 262–275, https://doi.org/10.1016/0033-5894(89)90093-8.

Benson, L.V., Currey, D.R., Dorn, R.I., Lajoie, K.R., Oviatt, C.G., Robinson, S.W., Smith, G.I., and Stine, S., 1990, Chronology of expansion and contraction of four great Basin lake systems during the past 35,000 years: Palaeogeography, Palaeoclimatology, Palaeoecology, v. 78, p. 241–286, https://doi.org/10.1016/0031-0182(90)90217-U.

Benson, L.V., Lund, S.P., Burdett, J.W., Kashgarian, M., Rose, T.P., Smoot, J.P., and Schwartz, M., 1998, Correlation of late-Pleistocene lake-level oscillations in Mono Lake, California, with North Atlantic climate events: Quaternary Research, v. 49, p. 1–10, https://doi.org/10.1006/qres.1997.1940.

Bereiter, B., Lüthi, D., Siegrist, M., Schüpbach, S., Stocker, T.F., and Fischer, H., 2012, Mode change of millennial CO_2 variability during the last glacial cycle associated with a bipolar marine carbon seesaw: Proceedings of the National Academy of Sciences of the United States of America, v. 109, p. 9755–9760, https://doi.org/10.1073/pnas.1204069109.

Bereiter, B., Eggleston, S., Schmitt, J., Nehrbass-Ahles, C., Stocker, T.F., Fischer, H., Kipfstuhl, S., and Chappellaz, J., 2015, Revision of the EPICA Dome C CO_2 record from 800 to 600-kyr before present: Geophysical Research Letters, v. 42, p. 542–549, https://doi.org/10.1002/2014GL061957.

Berger, A., and Loutre, M.F., 1991, Insolation values for the climate of the last 10 million years: Quaternary Science Reviews, v. 10, p. 297–317, https://doi.org/10.1016/0277-3791(91)90033-Q.

Bevilacqua, A., Bursik, M., Patra, A., Bruce Pitman, E., Yang, Q., Sangani, R., and Kobs-Nawotniak, S., 2018, Late Quaternary eruption record and probability of future volcanic eruptions in the Long Valley volcanic region (CA, USA): Journal of Geophysical Research: Solid Earth, v. 123, p. 5466–5494, https://doi.org/10.1029/2018JB015644.

Bischoff, J.L., Fitts, J.P., and Fitzpatrick, J.A., 1997, Responses of sediment geochemistry to climate change in Owens Lake sediment: An 800-k.y. record of saline/fresh cycles in core OL-92, *in* Smith, G.I., and Bischoff, J.L., eds., An 800,000-Year Paleoclimatic Record from Core OL-92, Owens Lake, Southeast California: Geological Society of America Special Paper 317, p. 37–47, https://doi.org/10.1130/0-8137-2317-5.37.

Bond, G., Broecker, W., Johnsen, S., McManus, J., Labeyrie, L., Jouzel, J., and Bonani, G., 1993, Correlations between climate records from North Atlantic sediments and Greenland ice: Nature, v. 365, p. 143–147, https://doi.org/10.1038/365143a0.

Cai, Y., et al., 2015, Variability of stalagmite-inferred Indian monsoon precipitation over the past 252,000 y: Proceedings of the National Academy of Sciences of the United States of America, v. 112, p. 2954–2959, https://doi.org/10.1073/pnas.1424035112.

Cassata, W.S., Singer, B.S., Liddicoat, J.C., and Coe, R.S., 2010, Reconciling discrepant chronologies for the geomagnetic excursion in the Mono Basin, California: Insights from new $^{40}Ar/^{39}Ar$ dating experiments and a revised relative paleointensity correlation: Quaternary Geochronology, v. 5, p. 533–543, https://doi.org/10.1016/j.quageo.2010.02.001.

Cheng, H., Lawrence Edwards, R., Shen, C.C., Polyak, V.J., Asmerom, Y., Woodhead, J., Hellstrom, J., Wang, Y., Kong, X., Spötl, C., Wang, X., and Alexander, E.C., 2013, Improvements in ^{230}Th dating, ^{230}Th and ^{234}U half-life values, and U-Th isotopic measurements by multi-collector inductively coupled plasma mass spectrometry: Earth and Planetary Science Letters, v. 371–372, p. 82–91, https://doi.org/10.1016/j.epsl.2013.04.006.

Chiang, H.W., Lu, Y., Wang, X., Lin, K., and Liu, X., 2019, Optimizing MC-ICP-MS with SEM protocols for determination of U and Th isotope ratios and ^{230}Th ages in carbonates: Quaternary Geochronology, v. 50, p. 75–90, https://doi.org/10.1016/j.quageo.2018.10.003.

Cobbold, P.R., Zanella, A., Rodrigues, N., and Løseth, H., 2013, Bedding-parallel fibrous veins (beef and cone-in-cone): Worldwide occurrence and possible significance in terms of fluid overpressure, hydrocarbon generation and mineralization: Marine and Petroleum Geology, v. 43, p. 1–20, https://doi.org/10.1016/j.marpetgeo.2013.01.010.

Cohen, A.S., Palacios-Fest, M.R., Negrini, R.M., Wigand, P.E., and Erbes, D.B., 2000, A paleoclimate record for the past 250,000 years from Summer Lake, Oregon, USA: II. Sedimentology, paleontology and geochemistry: Journal of Paleolimnology, v. 24, p. 151–182, https://doi.org/10.1023/A:1008165326401.

Colgan, J.P., and Henry, C.D., 2009, Rapid middle Miocene collapse of the Mesozoic orogenic plateau in north-central Nevada: International Geology Review, v. 51, p. 920–961, https://doi.org/10.1080/00206810903056731.

Deplazes, G., Lückge, A., Peterson, L.C., Timmermann, A., Hamann, Y., Hughen, K.A., Röhl, U., Laj, C., Cane, M.A., Sigman, D.M., and Haug, G.H., 2013, Links between tropical rainfall and North Atlantic climate during the last glacial period: Nature Geoscience, v. 6, p. 213–217, https://doi.org/10.1038/ngeo1712.

Dickinson, W.R., 2013, Phanerozoic palinspastic reconstructions of great basin geotectonics (Nevada-Utah, USA): Geosphere, v. 9, p. 1384–1396, https://doi.org/10.1130/GES00888.1.

Doughty, A.M., Kaplan, M.R., Peltier, C., and Barker, S., 2021, A maximum in global glacier extent during MIS 4: Quaternary Science Reviews, v. 261, no. 106948, https://doi.org/10.1016/j.quascirev.2021.106948.

Edwards, L.R., Chen, J.H., and Wasserburg, G.J., 1987, $^{238}U^{234}U^{230}Th^{232}Th$ systematics and the precise measurement of time over the past 500,000 years: Earth and Planetary Science Letters, v. 81, p. 175–192, https://doi.org/10.1016/0012-821X(87)90154-3.

Gilbert, G.K., 1890, Lake Bonneville: U.S. Geological Survey Monograph 1, 438 p., https://doi.org/10.3133/m1.

Gilbert, C.M., Christensen, M.N., Al-Rawi, Y., and Lajoie, K.R., 1968, Structural and Volcanic History of Mono Basin, California-Nevada: Geological Society of America Memoir 116, p. 275–329, https://doi.org/10.1130/MEM116-p275.

Hajdas, I., Bonani, G., Zimmerman, S.H., Mendelson, M., and Hemming, S., 2004, ^{14}C ages of ostracodes from Pleistocene lake sediments of the western Great Basin, USA—Results of progressive acid leaching: Radiocarbon, v. 46, p. 189–200, https://doi.org/10.1017/S0033822200039515.

Imbrie, J., Mix, A.C., and Martinson, D.G., 1993, Milankovitch theory viewed from Devils Hole: Nature, v. 363, p. 531–533, https://doi.org/10.1038/363531a0.

Jaffey, A.H., Flynn, K.F., Glendenin, L.E., Bentley, W.C., and Essling, A.M., 1971, Precision measurement of half-lives and specific activities of ^{235}U and ^{238}U: Physical Review C, v. 4, p. 1889–1906, https://doi.org/10.1103/PhysRevC.4.1889.

Jettestuen, E., Jamtveit, B., Podladchikov, Y.Y., deVilliers, S., Amundsen, H.E.F., and Meakin, P., 2006, Growth and characterization of complex mineral surfaces: Earth and Planetary Science Letters, v. 249, p. 108–118, https://doi.org/10.1016/j.epsl.2006.06.045.

Kaufman, D.S., Forman, S.L., and Bright, J., 2001, Age of the Cutler Dam Alloformation (Late Pleistocene), Bonneville basin, Utah: Quaternary Research, v. 56, p. 322–334, https://doi.org/10.1006/qres.2001.2275.

Kent, D.V., Hemming, S.R., and Turrin, B.D., 2002, Laschamp excursion at Mono Lake?: Earth and Planetary Science Letters, v. 197, p. 151–164, https://doi.org/10.1016/S0012-821X(02)00474-0.

Kleman, J., Fastook, J., Ebert, K., Nilsson, J., and Caballero, R., 2013, Pre-LGM Northern Hemisphere ice sheet topography: Climate of the Past, v. 9, p. 2365–2378, https://doi.org/10.5194/cp-9-2365-2013.

Kurth, G., Phillips, F.M., Reheis, M.C., Redwine, J.L., and Paces, J.B., 2011, Cosmogenic nuclide and uranium-series dating of old, high shorelines in the western Great Basin, USA: Bulletin of the Geological Society of America, v. 123, p. 744–768, https://doi.org/10.1130/B30010.1.

Laj, C., Kissel, C., Mazaud, A., Channell, J.E.T., and Beer, J., 2000, North Atlantic palaeointensity stack since 75 ka (NAPIS-75) and the duration of the Laschamp event: Philosophical Transactions of the Royal Society A: Mathematical, Physical, and Engineering Sciences, v. 358, p. 1009–1025, https://doi.org/10.1098/rsta.2000.0571.

Laj, C., Kissel, C., and Beer, J., 2004, High Resolution Global Paleointensity Stack since 75 kyr (GLOPIS-75) Calibrated to Absolute Values: Washington, DC, American Geophysical Union, Geophysical Monograph Series, v. 145, p. 255–265, https://doi.org/10.1029/145GM19.

Lajoie, K.R., 1968, Late Quaternary stratigraphic and geologic history of Mono Basin, eastern California [Ph.D. thesis]: Berkeley, California, USA, University of California, 271 p.

Lisiecki, L.E., and Raymo, M.E., 2005, A Pliocene-Pleistocene stack of 57 globally distributed benthic $\delta^{18}O$ records: Paleoceanography, v. 20, p. 1–17, https://doi.org/10.1029/2004PA001071.

Long, S.P., 2019, Geometry and magnitude of extension in the Basin and Range Province (39°N), Utah, Nevada, and California, USA: Constraints from a province-scale cross section: Bulletin of the Geological Society of America, v. 131, p. 99–119, https://doi.org/10.1130/B31974.1.

Löfverström, M., Caballero, R., Nilsson, J., and Kleman, J., 2014, Evolution of the large-scale atmospheric circulation in response to changing ice sheets over the last glacial cycle: Climate of the Past, v. 10, p. 1453–1471, https://doi.org/10.5194/cp-10-1453-2014.

Marcaida, M., Mangan, M.T., Vazquez, J.A., Bursik, M., and Lidzbarski, M.I., 2014, Geochemical fingerprinting of Wilson Creek formation tephra layers (Mono Basin, California) using titanomagnetite compositions: Journal of Volcanology and Geothermal Research, v. 273, p. 1–14, https://doi.org/10.1016/j.jvolgeores.2013.12.008.

Marcaida, M., Vazquez, J.A., Stelten, M.E., and Miller, J.S., 2019, Constraining the early eruptive history

of the Mono Craters rhyolites, California, based on ^{238}U-^{230}Th isochron dating of their explosive and effusive products: Geochemistry, Geophysics, Geosystems, v. 20, p. 1539–1556, https://doi.org/10.1029/2018GC008052.

Marcott, S.A., Bauska, T.K., Buizert, C., Steig, E.J., Rosen, J.L., Cuffey, K.M., Fudge, T.J., Severinghaus, J.P., Ahn, J., Kalk, M.L., McConnell, J.R., Sowers, T., Taylor, K.C., White, J.W.C., and Brook, E.J., 2014, Centennial-scale changes in the global carbon cycle during the last deglaciation: Nature, v. 514, p. 616–619, https://doi.org/10.1038/nature13799.

Meng, Q., Hooker, J., and Cartwright, J., 2018, Displacive widening of calcite veins in shale: Insights into the force of crystallization: Journal of Sedimentary Research, v. 88, p. 327–343, https://doi.org/10.2110/jsr.2018.18.

Menking, J.A., 2019, Stable isotope constraints on carbon dioxide and nitrous oxide variations at the onset of the Last Glacial Period: New ice core records from Taylor Glacier, Antarctica [Ph.D. thesis]: Corvallis, Oregon, USA, Oregon State University, 274 p.

Menking, K.M., Bischoff, J.L., Fitzpatrick, J.A., Burdette, J.W., and Rye, R.O., 1997, Climatic/hydrologic oscillations since 155,000 yr B.P. at Owens Lake, California, reflected in abundance and stable isotope composition of sediment carbonate: Quaternary Research, v. 48, p. 58–68, https://doi.org/10.1006/qres.1997.1898.

Menking, J.A., Brook, E.J., Shackleton, S.A., Severinghaus, J.P., Dyonisius, M.N., Petrenko, V., McConnell, J.R., Rhodes, R.H., Bauska, T.K., Baggenstos, D., Marcott, S., and Barker, S., 2019, Spatial pattern of accumulation at Taylor Dome during Marin Isotope Stage 4: Stratigraphic constraints from Taylor Glacier: Climate of the Past Discussions, v. 15, p. 1537–1556, https://doi.org/10.5194/cp-15-1537-2019.

Moseley, G.E., Edwards, R.L., Wendt, K.A., Cheng, H., Dublyansky, Y., Lu, Y., Boch, R., and Spotl, C., 2016, Reconciliation of the Devils Hole climate record with orbital forcing: Science, v. 351, p. 165–168, https://doi.org/10.1126/science.aad4132.

Oviatt, C.G., 2015, Chronology of Lake Bonneville, 30,000 to 10,000 yr B.P: Quaternary Science Reviews, v. 110, p. 166–171, https://doi.org/10.1016/j.quascirev.2014.12.016.

Oviatt, C.G., and McCoy, W.D., 1992, Early Wisconsin lakes and glaciers in the Great Basin, USA, *in* Clark, P.U., and Lea, P.D., The Last Interglacial-Glacial Transition in North America: Geological Society of America Special Paper 270, p. 279–287, https://doi.org/10.1130/SPE270-p279.

Oviatt, C.G., McCoy, W.D., and Reider, R.G., 1987, Evidence for a shallow early or middle Wisconsin-age lake in the Bonneville Basin, Utah: Quaternary Research, v. 27, p. 248–262, https://doi.org/10.1016/0033-5894(87)90081-0.

Peltier, C., Kaplan, M.R., Birkel, S.D., Soteres, R.L., Sagredo, E.A., Aravena, J.C., Araos, J., Moreno, P.I., Schwartz, R., and Schaefer, J.M., 2021, The large MIS 4 and long MIS 2 glacier maxima on the southern tip of South America: Quaternary Science Reviews, v. 262, no. 106858, https://doi.org/10.1016/j.quascirev.2021.106858.

Piotrowski, A.M., Goldstein, S.L., Hemming, S.R., and Fairbanks, R.G., 2005, Temporal relationship of carbon cycling and ocean circulation at glacial boundaries: Science, v. 307, p. 1933–1938, https://doi.org/10.1126/science.1104883.

Richards, D.A., and Dorale, J.A., 2003, Uranium-series chronology and environmental applications of speleothems: Uranium-series Geochemistry, v. 52, p. 407–460, https://doi.org/10.1515/9781501509308-015.

Russell, I.C., 1884, A geological reconnaissance in southern Oregon: U.S. Geologic Survey Annual Report, v. 4, p. 431–465.

Russell, I.C., 1889, Quaternary history of Mono Valley, California: U.S. Geological Survey Annual Report, v. 8, p. 261–394.

Russell, I.C., 1895, Present of Extinct Lakes of Nevada: New York, American Book Company, p. 101–132.

Schaefer, J.M., et al., 2015, The Southern Glacial Maximum 65,000 years ago and its Unfinished Termination: Quaternary Science Reviews, v. 114, p. 52–60, https://doi.org/10.1016/j.quascirev.2015.02.009.

Schneider, R., Schmitt, J., Köhler, P., Joos, F., and Fischer, H., 2013, A reconstruction of atmospheric carbon dioxide and its stable carbon isotopic composition from the penultimate glacial maximum to the last glacial inception: Climate of the Past, v. 9, p. 2507–2523, https://doi.org/10.5194/cp-9-2507-2013.

Seguinot, J., Rogozhina, I., Stroeven, A.P., Margold, M., and Kleman, J., 2016, Numerical simulations of the Cordilleran ice sheet through the last glacial cycle: The Cryosphere, v. 10, p. 639–664, https://doi.org/10.5194/tc-10-639-2016.

Stine, S., 1987, Mono Lake: The past 4,000 years [Ph.D. thesis]: Berkeley, California, USA, University of California, 732 p.

Stokes, C.R., Tarasov, L., and Dyke, A.S., 2012, Dynamics of the North American Ice Sheet Complex during its inception and build-up to the Last Glacial Maximum: Quaternary Science Reviews, v. 50, p. 86–104, https://doi.org/10.1016/j.quascirev.2012.07.009.

Szabo, B.J., 1990, Ages of travertine deposits in eastern Grand Canyon National Park, Arizona: Quaternary Research, v. 34, p. 24–32, https://doi.org/10.1016/0033-5894(90)90070-2.

Szabo, B.J., Kolesar, P.T., Riggs, A.C., Winograd, I.J., and Ludwig, K.R., 1994, Paleoclimatic inferences from a 120,000-yr calcite record of water-table fluctuation in Browns Room of Devils Hole, Nevada: Quaternary Research, v. 41, p. 59–69, https://doi.org/10.1006/qres.1994.1007.

Szabo, B.J., Bush, C.A., and Benson, L.V., 1996, Uranium-series dating of carbonate (tufa) deposits associated with quaternary fluctuations of Pyramid Lake, Nevada: Quaternary Research, v. 45, p. 271–281, https://doi.org/10.1006/qres.1996.0028.

Tulenko, J.P., Lofverstrom, M., and Briner, J.P., 2020, Ice sheet influence on atmospheric circulation explains the patterns of Pleistocene Alpine glacier records in North America: Earth and Planetary Science Letters, v. 534, no. 116115, https://doi.org/10.1016/j.epsl.2020.116115.

Vazquez, J.A., and Lidzbarski, M.I., 2012, High-resolution tephrochronology of the Wilson Creek Formation (Mono Lake, California) and Laschamp event using ^{238}U–^{230}Th SIMS dating of accessory mineral rims: Earth and Planetary Science Letters, v. 357–358, p. 54–67, https://doi.org/10.1016/j.epsl.2012.09.013.

Vincent, J.-S., and Prest, V.K., 1987, The Early Wisconsinan History of the Laurentide Ice Sheet: Géographie physique et Quaternaire, v. 41, p. 199–213, https://doi.org/10.7202/032679ar.

Wang, Y., Cheng, H., Edwards, R.L., Kong, X., Shao, X., Chen, S., Wu, J., Jiang, X., Wang, X., and An, Z., 2008, Millennial- and orbital-scale changes in the East Asian monsoon over the past 224,000 years: Nature, v. 451, p. 1090–1093, https://doi.org/10.1038/nature06692.

Wang, Y.J., 2001, A high-resolution absolute-dated late Pleistocene monsoon record from Hulu Cave, China: Science, v. 294, p. 2345–2348, https://doi.org/10.1126/science.1064618.

Wendt, K.A., Dublyansky, Y.V., Moseley, G.E., Edwards, R.L., Cheng, H., and Spötl, C., 2018, Moisture availability in the southwest United States over the last three glacial-interglacial cycles: Science Advances, v. 4, no. eaau1375, https://doi.org/10.1126/sciadv.aau1375.

Winograd, I.J., Szabo, B.J., Coplen, T.B., and Riggs, A.C., 1988, A 250,000-year climatic record from great basin vein calcite: Implications for Milankovitch theory: Science, v. 242, p. 1275–1280, https://doi.org/10.1126/science.242.4883.1275.

Winograd, I.J., Coplen, T.B., Landwehr, J.M., Riggs, A.C., Ludwig, K.R., Szabo, B.J., Kolesar, P.T., and Revesz, K.M., 1992, Continuous 500,000-year climate record from vein calcite in Devils Hole, Nevada: Science, v. 258, p. 255–260, https://doi.org/10.1126/science.258.5080.255.

Winograd, I.J., Landwehr, J.M., Coplen, T.B., Sharp, W.D., Riggs, A.C., Ludwig, K.R., and Kolesar, P.T., 2006, Devils Hole, Nevada, $\delta^{18}O$ record extended to the mid-Holocene: Quaternary Research, v. 66, p. 202–212, https://doi.org/10.1016/j.yqres.2006.06.003.

Zimmerman, S.H., Hemming, S.R., Kent, D.V., and Searle, S.Y., 2006, Revised chronology for late Pleistocene Mono Lake sediments based on paleointensity correlation to the global reference curve: Earth and Planetary Science Letters, v. 252, p. 94–106, https://doi.org/10.1016/j.epsl.2006.09.030.

Zimmerman, S.R.H., Steponaitis, E., Hemming, S.R., and Zermeño, P., 2012, Potential for accurate and precise radiocarbon ages in deglacial-age lacustrine carbonates: Quaternary Geochronology, v. 13, p. 81–91, https://doi.org/10.1016/j.quageo.2012.07.003.

Science Editor: Brad S. Singer
Associate Editor: Emmanuel Gabet

Manuscript Received 16 February 2021
Revised Manuscript Received 28 May 2021
Manuscript Accepted 29 October 2021

Printed in the USA